Author(s): Lehtonen, Suvi-Maaria; Puumalainen, Veera; Nokia, Miriam S.; Lensu, Sanna

Title: Effects of unilateral hippocampal surgical procedures needed for calcium imaging on mouse behavior and adult hippocampal neurogenesis

Year: 2024

Version: Published version

Please cite the original version:

Lehtonen, S.-M., Puumalainen, V., Nokia, M. S., & Lensu, S. (2024). Effects of unilateral hippocampal surgical procedures needed for calcium imaging on mouse behavior and adult hippocampal neurogenesis. Behavioural Brain Research, 468, Article 115042. https://doi.org/10.1016/j.bbr.2024.115042

Behavioural Brain Research 468 (2024) 115042

Contents lists available at ScienceDirect

Behavioural Brain Research

journal homepage: www.elsevier.com/locate/bbr

Effects of unilateral hippocampal surgical procedures needed for calcium imaging on mouse behavior and adult hippocampal neurogenesis

Suvi-Maaria Lehtonen *, Veera Puumalainen, Miriam S. Nokia, Sanna Lensu

Department of Psychology and Centre for Interdisciplinary Brain Research, University of Jyvaskyla, Finland

ARTICLE INFO

Keywords:
Adeno-associated viral vector
Adult hippocampal neurogenesis
Calcium imaging
Dentate gyrus
GCaMP

ABSTRACT

Hippocampus is essential for episodic memory formation, lesion studies demonstrating its role especially in processing spatial and temporal information. Further, adult hippocampal neurogenesis (AHN) in the dentate gyrus (DG) has also been linked to learning. To study hippocampal neuronal activity during events like learning, *in vivo* calcium imaging has become increasingly popular. It relies on the use of adeno-associated viral (AAV) vectors, which seem to lead to a decrease in AHN when applied on the DG. More notably, imaging requires the implantation of a relatively large lens into the tissue. Here, we examined how injection of an AAV vector and implantation of a 1-mm-diameter lens into the dorsal DG routinely used to image calcium activity impact the behavior of adult male C57BL/6 mice. To this aim, we conducted open-field, object-recognition and object-location tasks at baseline, after AAV vector injection, and after lens implantation. Finally, we determined AHN from hippocampal slices using a doublecortin-antibody. According to our results, the operations needed for *in vivo* imaging of the dorsal DG did not have adverse effects on behavior, although we noticed a decrease in AHN ipsilaterally to the operations. Thus, our results suggest that *in vivo* imaging can be safely used to, for example, correlate patterns of calcium activity with learned behavior. One should still keep in mind that the defects on the operated side might be functionally compensated by the (hippocampus in the) contralateral hemisphere.

1. Introduction

Episodic memory refers to multimodal memories of personally experienced events. The hippocampus is essential for encoding, consolidation and retrieval of episodic memories [36,40]. Dentate gyrus (DG), the input region of the hippocampus and the one region producing new neurons also in adults, is thought to be necessary for spatial and contextual pattern separation [30]. This process ensures the fidelity of memories and is suggested to be enhanced by adult hippocampal neurogenesis (AHN) [10,33].

Studies concerning the role of the hippocampus in learning and those regarding the contribution of AHN to cognition have mostly been conducted by manipulating the brain bilaterally. For example, bilateral hippocampal lesions seem to impair spatial learning [12,26,27] but not object recognition memory [13,27]. Evidence suggesting a role for AHN in learning has emerged from studies in which AHN has been disrupted either chemically or by irradiation: Adult-born immature granule cells seem to be critical for encoding spatial and temporal information (for a review, see Anacker & Hen 2017), and a decrease in AHN has been linked to impaired object-location memory in rodents, whereas the memory for object identity (recognition of familiar vs. novel objects) remains intact [17,23]. Research on the effects of unilateral lesions or unilateral manipulation of AHN is rare, if existent at all. It has been suggested that abnormal activity in the hippocampus due to a medial septal lesion might be behaviorally more detrimental than lesioning the whole hippocampus [rabbit: [5]].

Knowledge on the effects of unilateral manipulations of the hippocampus is much needed as current imaging methods, such as *in vivo* calcium (Ca^{2+}) imaging in freely moving rodents, involves highly invasive procedures most often targeted to the hippocampus unilaterally. Ca^{2+} imaging has proven especially useful for studying DG neurons [1,22,37,41], as there cells seldom fire action potentials and can thus be hard to capture with traditional extracellular electrophysiological single-unit recordings. The basic idea in Ca^{2+} imaging is to monitor

Abbreviations: AAV vector, Adeno-associated viral vector; AHN, adult hippocampal neurogenesis; CaMKII, Calcium/calmodulin-dependent kinase II; DG, dentate gyrus; GECI, genetically encoded calcium indicator; GFP, green fluorescent protein; GRIN, gradient refractive index lens; NOR, novel-object recognition; OF, open field; OL, object-location.

* Corresponding author.
E-mail address: lehtsu@jyu.fi (S.-M. Lehtonen).

https://doi.org/10.1016/j.bbr.2024.115042
Received 13 November 2023; Received in revised form 17 April 2024; Accepted 3 May 2024
Available online 7 May 2024

enhanced free Ca^{2+} ion concentration during increased neural activity. To capture fluctuations in Ca^{2+} concentration, genetically encoded calcium indicators (GECIs) such as those from the GCaMP family are used [28]. GECIs are transferred into the target cells typically using a recombinant adeno-associated virus (AAV) vector [19,21]. While the use of AAV vectors in intracerebral gene transfer is considered safe, and they cause none or only a mild immune response in rodents [18,3], one study suggests AAV vectors to decrease AHN in a dose-dependent manner with doses relevant to experimental use [20]. Related, cytotoxicity of the GCaMP and its buffering effect on the intracellular Ca^{2+} activity could impact calcium-dependent processes related to cellular signaling and synaptic potentiation in the target cells [25,38]. Finally, the $\leq$ 1 mm-diameter lens needed for imaging [19] generates a nonspecific lesion not only to the target area but also to the tissue above it, including areas of the parietal cortex, the cingulum, the corpus callosum and the alveus, and if the DG is imaged, also the CA1 [see for example [12,24,6]]. Taken together, these facts raise concern of disrupting brain function and behavior whilst performing *in vivo* imaging. Yet, there seem to be very few studies directly addressing this issue, especially regarding the hippocampus.

Here, we explored whether first injecting a viral system carrying a GECI and then chronically implanting a lens into the dorsal hippocampus impacts the behavior of adult male C57BL/6 mice, in comparison to sham-operated or unoperated control mice. To this end, we carried out open field (OF), novel object recognition (NOR) and object-location (OL) tasks at baseline, after injecting the viral system, and after implanting the lens. After ~6 months, the mice were sacrificed, and the brains of operated groups were analyzed histologically. Adult-born DG granule cells were identified with a doublecortin-antibody and the amount of green fluorescence (GF) was analyzed to confirm the expression of the viral system in the hippocampus. We expected to see a decrease in AHN ipsi- but not contralaterally to the operations [20]. We also assumed that this together with the lens-induced lesion to the neocortex and the dorsal CA1 could have adverse effects on performance on the OL but not on the NOR task [12,17,23,26,27]. However, because both the injection and lesion were unilateral, leaving the contralateral hippocampus intact, we anticipated the effects to be modest. Finally, we expected to see progressively better learning in the NOR and in the OL task as a function of repetition [29].

2. Materials and methods

2.1. Ethics statement

All experimental procedures were approved by the Animal Experiment Board of Southern Finland (license ESAVI-24666/2018) and implemented in accordance with directive 2010/63/EU of the European Parliament and of the Council on the care and use of animals for research purposes. Experiments were carried out in the Laboratory center at the University of Jyväskylä.

2.2. Animals

We used 28 male mice (C57Bl/6JRccHsd from Envigo, Netherlands) aged 7.8 ± 0.2 weeks and weighing 25.9 ± 2.0 g (mean ± standard deviation) at the time of the first surgery. We divided the mice into three groups: experimental (GCaMP, n = 14), sham-operated (PBS, n = 6), and control (n = 8). Prior to surgery, the mice were housed in groups of four, and thereafter in pairs or triplets. Standard mouse cages (Tecniplast Eurostandard type II, 268 ×215×141 mm) made of transparent plastic were used. Food (R36, Lantmännen, Stockholm, Sweden) and water was available *ad libitum*, and room temperature was controlled at 21 ± 2°C and humidity at 50 ± 10%. The mice had aspen chips and fiber (Tapvei, Estonia) together with paper towels as bedding and nesting material, and cardboard tubes as enrichment. The mice were maintained on a 12:12-hour light-dark cycle, with lights on at 8 am. Surgical operations and behavioral tests were carried out during the light portion of the cycle. Well-being of the animals was monitored daily, and they were weighed regularly. Before behavioral tests, the mice were familiarized with handling for 10 days, 5–10 minutes per animal each day. The control mice were neither anesthetized nor surgically operated but were handled like the GCaMP and PBS mice.

2.3. Viral construct

An AAV9 vector was used to carry a GCaMP6s calcium indicator gene with a Calcium / calmodulin-dependent kinase II (CaMKII) promoter into the DG. A ready-made construct AAV.CamKII.GCaMP6s.WPRE.SV40 was from Addgene (Addgene viral prep. # 107790-AAV9, a gift from James M. Wilson; http://n2t.net/addgene:107790-AAV9), and it was diluted at 1:8 into sterile PBS resulting in $3.5*10^9$ particles / ml. Based on recent studies using an AAV vector and a GCaMP6 calcium indicator with a CaMKII promoter, titers of ~$1.3–2.3*10^{13}$ viral particles / ml (total dose of $6–10*10^9$ viral particles per animal) generates optimal GCaMP expression in the hippocampus (see for example [2,41]). In the current study a lower dose (altogether $3.5*10^6$ viral particles per animal) was used to ensure that the expression would remain within optimal range for an extended period.

2.4. Surgery

Surgical procedures were modified from Allegra and colleagues [1] and Carrier-Ruiz and colleagues [8]. Mice were anesthetized with isoflurane and mounted in a stereotactic frame laying on a heated pad (+37 °C) to maintain body temperature. Eyes were protected with petrolatum (Valkovaseliini, Vitabalans oy, Hämeenlinna, Finland). Mice were injected with carprofen (5 mg/ml, 0.01 ml/10 g *s.c.,* Rimadyl VET, Zoetis, Denmark) before the surgery and for the following three to five days. Mice were liquefied with saline during operations, and before the lens implantation injected with corticosteroid (0.02 mg/ml, 0.2 mg/kg *s.c.*, Oradexon, Aspen, Denmark). Hair from the top of the skull was removed using Veet®, and the scalp was disinfected using povidone-iodine-ethanol (Betadine-EtOH).

2.4.1. Viral injection

A ~1.2 mm round hole was drilled above the DG, to allow both injection and, later, lens implantation. Injections were made using a pulled glass capillary (TW100F-4 OD 1.0 mm, WPI, Sarasota, USA) attached to a 5-μl Hamilton syringe secured in a programmable pump (Remote Infuse/Withdraw Pump 11 Elite Nanomite Programmable Syringe Pump, Harvard Apparatus, USA). The pump was attached to a stereotactic manipulator, operated manually. The injection rate was 100 nl/min, and the injection was always started already from the shallowest position so that there was pressure in the capillary when lowering it into the tissue. All animals received four 250-nl injections targeting the dorsal DG at 2 mm posterior and 0.9 and 1.4 mm lateral to bregma [31]. Injections in the same mediolateral position but at different depths (2.1 and 2.3 mm below dura) were performed without a delay, while the latter position was followed by a 10-minute waiting time before lifting the capillary from the brain. The dose of the viral construct was $0.875*10^6$ particles per injection site, equaling at $3.5*10^6$ viral particles per animal in the GCaMP group. The PBS group was injected similarly, but with sterile PBS. Half of the mice received injections to the left and half to the right hippocampus. At the end of the surgery, the wound was sutured.

2.4.2. Lens implantation

Two to three weeks after the viral injection, a lens was implanted above the injection site in the DG. For the implantation of the integrated GRIN-lens (diameter 1 mm, length 4 mm, #1050–004637, Inscopix, Mountain View, CA, USA) or a similar dummy lens (#1050–002920, Inscopix) we used the same hole as for the injections. Additional holes

were drilled for two or three screws (#BN406, Bossard, Bossard Holding AG, Zug, Switzerland), which helped secure the lens to the skull. Before implantation, we made a tract for the lens with a blunted glass capillary (diameter 1 mm) according to the protocol by Allegra et al. Allegra et al., [1]. The capillary was lowered at 10 μm/s using a motorized programmable stereotactic manipulator (Scientifica LinLab2, Judges Scientific plc, UK) to reach the target at 2.2 mm below the dura. Next, we lowered the lens in place at a speed of 1.7 μm/s, positioning the center at 2 mm posterior and 1.15 mm lateral to bregma. The final depth of the lens was determined based on fluorescence signal monitored during surgery (nVista, Inscopix). Finally, the lens was fixed in place with dental cement (SuperBond, Sun Medical Co, Shiga, Japan).

2.5. Behavioral tasks

The behavioral tasks were all conducted in the same room. The lighting in the room was kept dim and the researcher was present but quiet and out of sight in all experiments. After each session, the arena and objects were cleaned thoroughly with 70% ethanol. The experimental protocol is visualized in Fig. 1A. To investigate exploration, anxiety-related behavior, and learning, we conducted Open Field (OF), Novel Object Recognition (NOR), and Object-Location (OL) tasks. The learning tasks (NOR and OL) consisted of one training trial before a test trial. The tasks were conducted at three timepoints: Before the stereotactic operations (baseline, mice ~8–9 weeks old), after the AAV.CaMKII.GCaMP6s or PBS injection (injection, mice ~10–11 weeks old), and after the lens or dummy lens implantation (implant, mice ~13–14 weeks old). The mice were allowed at least a week of recovery from the operations before starting behavioral tasks, and at least 24 h between each individual task. The tasks were carried out according to a similar schedule in the unoperated control mice, and thus we refer to the three timepoints consistently as "baseline", "injection" and "implant". The last behavioral task, a 21-day contextual fear discrimination, was carried out accompanied by DG calcium imaging, but these data are to be reported elsewhere.

2.5.1. Open field (OF)

First, to measure behavior indicative of anxiety and locomotor activity and to habituate the mice to the environment, we carried out an OF task. Before the task, the mice (GCaMP: n = 14; PBS: n = 6; control: n = 8) were let to acclimate for 30 min to a single cage in a quiet space next to the experimental room. Then, the mouse was carried in its cage into the experimental room and lifted with a cardboard tube and placed into the middle of an empty plywood arena. The arena was dark brown (L 50 cm x W 50 cm x H 32 cm) and the floor was covered with either black plastic or a light grey Lego™ sheet. The mouse was allowed to explore the area freely for 10 min and was then lifted back to an individual cage with a tube and allowed to rest for 30 min, before returning it to the home cage.

2.5.2. Novel object recognition (NOR)

When exposed to familiar and novel objects, rodents tend to spend more time exploring the novel than the familiar one, suggesting that they retain a representation of the familiar object in memory. This type

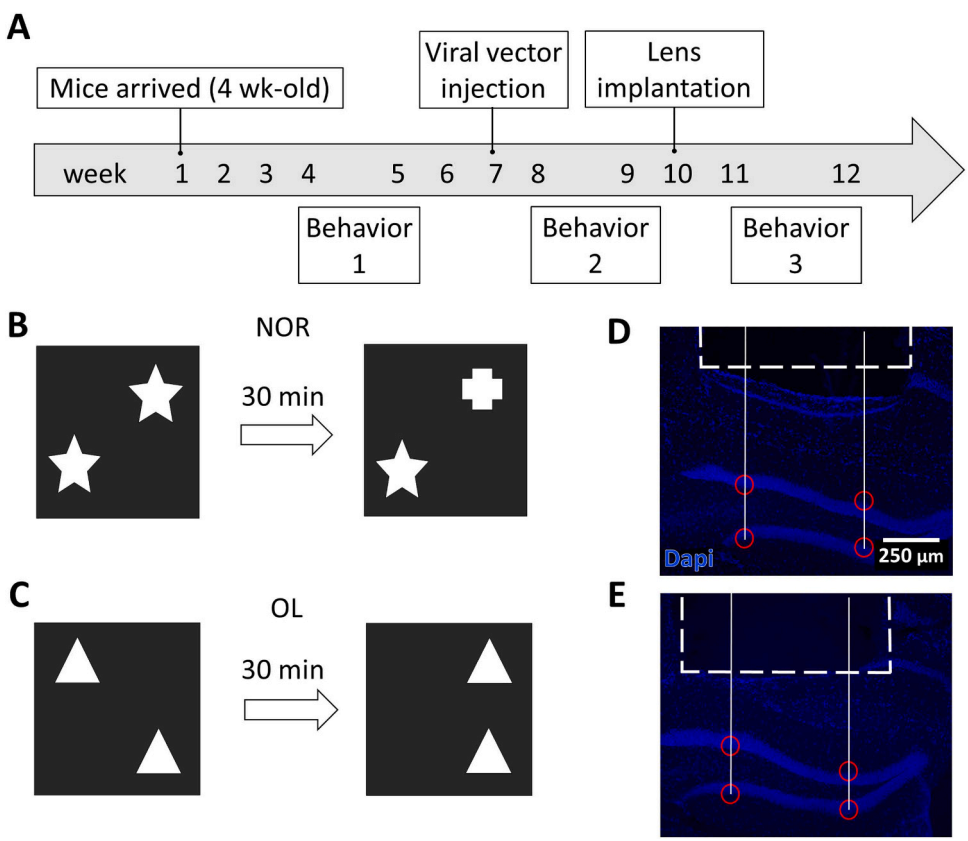

Fig. 1. Experimental protocol. A) Timeline for the stereotactic operations and behavioral tests. In the first operation, an AAV9 vector carrying CaMKII.GCaMP6s calcium indicator gene was injected into the DG. After a ~3-week recovery, a 1-mm GRIN lens was implanted into the same region. Behavioral tests were carried out prior to operations (Behavior 1), after AAV.CaMKII.GCaMP6 injection (Behavior 2), and after lens implantation (Behavior 3), with ~1 week recovery from the operations. Sham-treated controls (PBS-group) were injected with PBS and implanted with a dummy lens, at corresponding times. Unoperated control animals went through equal behavioral protocol without any surgical operations. Learning tasks consisted of B) an object recognition task and C) an object-location task. Inter-task interval was ~24 h. D) Lens position (dashed line) and the injection sites (red circles) from representative mice from the GCaMP group and E) the PBS group. The lenses were located ~350– 450 μm above the upper blade of the DG.

of novelty-preference in spontaneous exploratory behavior is used to study hippocampus-dependent "episodic-like" memory in rodents [11].

We conducted a one-trial NOR task [15] ~24 h after the OF task (Fig. 1B). The arena used in NOR was the same as in the OF task (black floor). During the training trial, two identical objects were placed in the arena ~10 cm from the edges and ~25 cm from each other. The objects were ~4–8 cm tall and made of plastic and/or metal. The mouse was placed in the arena and allowed to freely explore for 10 min. Then the mouse had a 30-min break in an individual cage. In a test trial the mouse was again allowed to explore the arena for 10 min. Now, one of the objects had been replaced with a novel object, which was easily distinguishable from the original objects yet shared a somewhat similar complexity with them. The locations of the objects remained the same as in the training trial. For each mouse, different objects were used at different time points (baseline, injection, and implant). The object locations were counterbalanced, and the use of objects as familiar and novel was rotated between animals.

2.5.3. Object-location (OL)

OL task was used to examine spatial memory, which is suggested to be another aspect of episodic-like memory [14]. The same environmental settings were used as described above regarding NOR, and the mice were handled in a similar way prior to and after the task. During the 10-min training trial the mouse was let to explore the arena containing two identical objects, which were placed in opposite corners ~10 cm from the edges. Then, the mice had a 30-min break in a standard cage (Fig. 1C). For the test trial, one of the objects was relocated to a different corner (rotated 45° to either direction), and the mouse was allowed to explore the arena again for 10 min. To make navigation easier, the mice were placed in the center of the arena always so that their nose was pointing to the same direction. The object locations were counterbalanced. To minimize the possibility that habituation to the test conditions could mix the results, we used different objects and locations on each timepoint (baseline, injection and implant). We also conducted the OL task using a longer, 24-h delay and different objects but the results are not reported as the mice did not learn the task.

2.5.4. Data and data analysis

The behavior of each mouse in each task was recorded at 25 fps using a Basler ace (acA1440–220uc, Germany) camera positioned on top of the arena and Pylon Viewer software. Behavior was scored offline by trained persons (undergraduate students) unaware of the identity of the mouse, and the score after 1, 5, and 10 min of exploration was recorded. After preliminary inspection it became obvious that the mice explored the objects in the OL and NOR tasks most consistently within the first 5 min (about novelty preference, see [14]) and hence the score at this timepoint was used in all analyses.

OF. A 4 ×4 grid was placed over the arena floor on the video, and the number of movements across a line and the number of rearings were recorded. In addition, the time (s) spent at the center of the arena (4 innermost squares of the grid) was recorded.

NOR and OL. From the behavioral videos, time (s) spent exploring the two objects was recorded. Exploration was defined as pointing the nose ≤ 1 cm from the object or making physical contact with it (sniffing, touching, climbing). Only sessions in which the mice explored both objects for at least 3 seconds were included in the analyses. A discrimination index indicating relative preference to either one of the objects was calculated: The time spent exploring the (to be) novel (NOR) or the (to be) moved (OL) object minus the time spent exploring the stable object was divided by that spent exploring either object. Thus, an index greater than zero indicates preference for the novel/moved object.

2.6. Histology and immunohistochemistry

The mice were injected with an overdose of pentobarbital (~130 mg/ml, Euthasol Vet, Dechra veterinary, Netherlands) and perfused with physiological saline (0.9%, Orion Pharma, Finland) followed by fresh 4% paraformaldehyde. After post-fixation in 4% paraformaldehyde overnight, the brain was washed with 0.1 M phosphate buffer and cryoprotected in 30% sucrose solution. Later, the brains were cut into 40-μm coronal sections using a sliding microtome (Leica SM 2010 R Microtome, Leica Instruments GmBH, Germany). The sections were collected into series of 12 Eppendorf tubes (2 ml) filled with cryoprotectant solution (30% sucrose and 30% ethylene glycol in 0.05 M phosphate buffer added with 0.025% w/v sodium azide, pH 7.6) and stored at −20 °C until staining.

To study AHN, free-floating sections were immunostained in room temperature using a shaker plate throughout the protocol. First, sections were washed with 1X PBS (pH 7.4) and blocked with goat serum (10% normal goat serum, Biowest #5200 H-500 in 1X PBS, supplemented with 0.3% Triton X-100, Electran Triton X-100, VWR 437002 A) for 30 minutes. Then the sections were incubated in the doublecortin (DCX) antibody (1:800, polyclonal produced in rabbit, Cell Signaling Technology, #4604) overnight. On the next day, the sections were first washed 3 ×10 min in PBS and then incubated in secondary antibody (Alexa Fluor 546 goat anti-rabbit IgG, Invitrogen by Thermo Fisher Scientific, #A11035, 1:200) for 2 hours, and then washed with PBS again. Both antibodies were diluted in PBS supplemented with 1% normal goat serum and 0.3% Triton X-100. Finally, the sections were mounted on clean objective slides and allowed to dry before coverslipping them with a mounting media including 4′,6-diamidino-2-phenylindole (DAPI, nuclei stain) (VectaShield® HardSet™ Antifade mounting media with DAPI, Vector Laboratories, #H-1500).

The location of the lens was assessed using the mouse brain atlas [31] as reference: In the GCaMP group the lens was located on average 340 μm above the upper blade of the dorsal DG (Fig. 1D–E). In the PBS group, the dummy lens was on average 420 μm above the upper blade of the DG. The expression of GCaMP was measured with GF intensity in both hemispheres. For the analysis we imaged three hippocampal sections with a confocal microscope (Zeiss LSM 700, 10x/NA 0.45, unidirectional scanning). One image was taken targeting the lens/dummy, one was taken anterior and one posterior to it (1.06–3.08 mm posterior to bregma). All images for the GF analysis were taken with the following settings: image size 1280.35 ×1280.35 μm (0.63 μm pixel size), laser power 0.40, pinhole 70.0, AU 2.14, gain 463, digital offset 0 and digital gain 1.0. Emission filters were short pass 555 for GFP and long pass 490 for DCX. From the image, the mean and maximum GF intensity values were measured with QuPath® version 0.4.2. using the software intensity feature detector for the green channel [4]. GF intensity was averaged over the three images to obtain one value per mouse.

DCX-positive cells with a neuron-like structure and a size of ~10 μm were counted in the dorsal DG including the hilus under a confocal microscope (Zeiss LSM 700, 20x/NA 0.8), from the same three sections which were imaged for the analysis of GF intensity (see above). To yield an estimate of AHN in each hemisphere, we calculated the sum of DCX-positive cells in the three sections. To investigate if the AAV9 construct affected AHN, we calculated the correlation between the GF intensity and the number of DCX-positive cells within each hemisphere.

2.7. Statistical analyses

The data was analyzed using IBM SPSS statistics 28. Within-subject changes in behavior (discrimination index) between the training and the test trial (learning) in the NOR and OL were analyzed using the Wilcoxon signed-rank test. Changes in performance in the OF, NOR and OL tasks across time (baseline, injection, implant) and differences between groups (GCaMP, PBS, control) were analyzed using Generalized Estimating Equations (GEE, linear model). The data was analyzed in long format, in which N is the number of mice x number of observations. Independent working correlation matrix was selected based on the Quasi-likelihood under the independence model criterion (QIC). Bonferroni-corrected p-values are reported for pairwise comparisons.

For the GF and AHN data, all within-subject analyses were conducted using the Wilcoxon signed-rank test and between-subjects analyses using the Mann-Whitney U test. Spearman's rank correlation coefficient (r_s) was used to analyze connections between variables.

3. Results

3.1. Surgical procedures affected exploration activity in the open field

Two of the 14 GCaMP mice died during the experiment, resulting in final group sizes of 12 for GCaMP, 6 for PBS, and 8 for the control group after implantation. There was a main effect of group in exploration behavior measured as the number of line crossings [GEE, group x timepoint interaction: Wald χ^2 (4, N = 82) = 7.12, p = 0.129; main effect of group: Wald χ^2 (2, N = 82) = 8.98, p = 0.011, and timepoint: Wald χ^2 (2, N = 82) = 5.26, p = 0.072] (Fig. 2A). Pairwise comparison (Bonferroni) revealed that the control group was more active ([mean ± standard deviation] 182 ± 7) throughout the experiment than the GCaMP group (152 ± 8, p = 0.018). There were no differences between the GCaMP and the PBS group (145 ± 19, p = 1.000) nor between the PBS and the control group (p = 0.209).

Rearing was different between the groups and between the timepoints [group x timepoint interaction: Wald χ^2 (4, N = 82) = 20.08, p < 0.001, main effect of group: Wald χ^2 (2, N = 82) = 98.80, p < 0.001 and timepoint: Wald χ^2 (2, N = 82) = 17.86, p < 0.001]. Pairwise comparisons revealed no difference in rearing between the GCaMP and the PBS groups at any timepoint (p = 0.309—1.000). The control group reared more than the GCaMP group at all timepoints (baseline: 52 ± 10 vs. 34 ± 12, p < 0.001; injection: 56 ± 9 vs. 22 ± 8, p < 0.001; implant: 53 ± 10 vs. 27 ± 12, p < 0.001). In addition, the control group reared more than the PBS group after injection and implantation (baseline: 52 ± 10 vs. 43 ± 8, p = 0.410; injection: 56 ± 9 vs. 22 ± 7, p < 0.001; implantation: 53 ± 10 vs. 25 ± 20, p = 0.006). Follow-up analyses (GEE separately for each group) revealed a change in rearing in the GCaMP [Wald χ^2 (2, N = 40) = 11.18, p = 0.004] and in the PBS [Wald χ^2 (2, N = 18) = 29.07, p < 0.001] groups but not in the control group [Wald χ^2 (2, N = 24) = 0.88, p = 0.643]. Rearing decreased across time, after surgical procedures, both in the GCaMP (baseline vs. injection: 34 ± 13 vs. 22 ± 8; p = 0.003) and in the PBS group (baseline vs. injection: 43 ± 8 vs. 22 ± 7; p < 0.001). (Fig. 2B).

There was a statistically significant interaction of group and timepoint in time spent in the center [Wald χ^2 (4, N = 82) = 19.60, p < 0.001], with no main effect of group [Wald χ^2 (2, N = 82) = 5.02, p = 0.081] but a statistically significant effect of timepoint [Wald χ^2 (2, N = 82) = 23.25, p < 0.001]. Pairwise comparisons indicated that the GCaMP group spent more time in the center at baseline than the PBS (p = 0.002) and the control (p = 0.010) group. There were no differences after injection (GCaMP vs. PBS: p = 1.000, GCaMP vs. control: p =

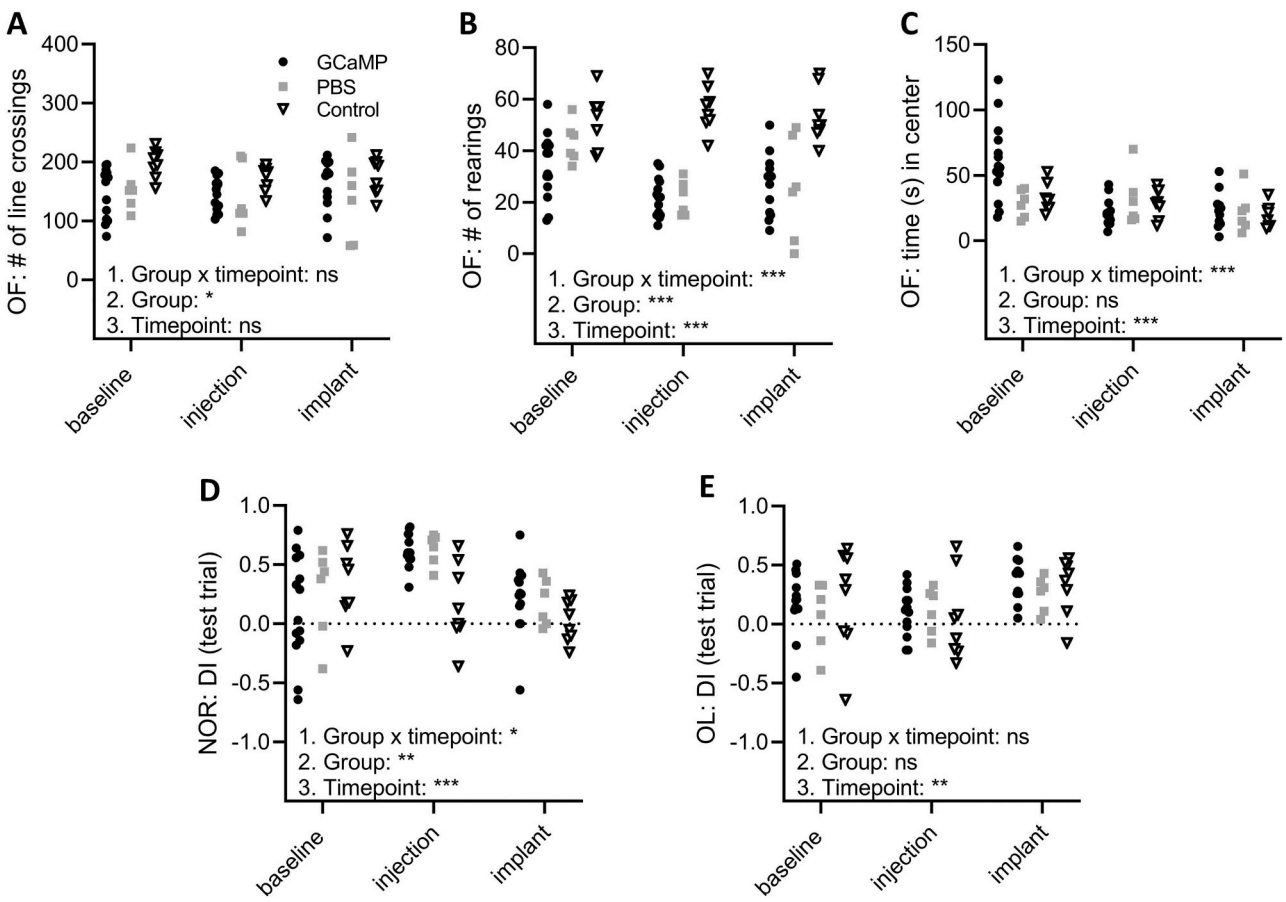

Fig. 2. The surgical operations impacted activity in the open field arena but did not impair short-term object-recognition (NOR) or object-location (OL) memory. Explorative activity in the open field arena (40 ×40 cm) was studied in three timepoints and the behavior was evaluated offline. A) A 4×4 grid was aligned above the recording enabling the calculation of number (#) of lines crossed, describing activity. Anxiety was measured as B) the number (#) of rearings, and C) time (s) spent in the center of the arena, formed by the four innermost squares of the grid. Results of D) NOR and E) OL tasks from the three timepoints. Discrimination indexes were calculated by subtracting the time spent exploring the stable object from the time spent exploring the novel or the moved object and dividing this by the total object exploration time. Higher positive values indicate better discrimination and negative values indicate that no discrimination occurred. In all panels, the individual observations are shown with black circles (GCaMP), grey squares (PBS), and clear triangles (Control). Asterisks refer to statistically significant differences in Generalized estimating equations: p < 0.050 (*), p ≤ 0.01 (**) and p < 0.001 (***).

0.828) and implantation (GCaMP vs. PBS: p = 1.000, GCaMP vs. control: p = 1.000), nor between the PBS and the control group at any timepoint (p = 0.402—0.770). Within-subjects analysis revealed a change in time spent in the center in the GCaMP [Wald χ^2 (2, N = 40) = 26.051, p < 0.001] and in the control [Wald χ^2 (2, N = 24) = 9.975, p = 0.007] group but not in the PBS [Wald χ^2 (2, N = 18) = 1.577, p = 0.454] group (Fig. 2C). The GCaMP group spent more time in the center at baseline (61 ± 30 s) than after injection (21 ± 10 s; p < 0.001) and after implantation of the lens (61 ± 30 s vs. 24 ± 14 s; p < 0.001). In the control group, there was a decrease in time spent in the center after implantation compared to the baseline (33 ± 11 s vs. 19 ± 9 s; p = 0.005).

3.2. The GCaMP and the PBS groups performed better at novel-object recognition after the injection

Results of the NOR task are presented in Fig. 2D. In the GCaMP group, discrimination indices revealed no learning (relative preference for the novel object) at baseline (One-sample Wilcoxon signed-rank test, Z = 0.97, p = 0.331), while after the injection (Z = 2.61, p < 0.001) and again after the implantation (Z = 2.20, p = 0.028) the GCaMP group learned the task. The PBS group learnt the task after injection (Z = 2.20, p = 0.028,) but not at baseline (Z = 1.57, p = 0.116) or after implantation (Z = 1.75, p = 0.080). The control group showed no learning at any of the timepoints (Z = 1.96 / 0.98 / 0.35, p = 0.050 / 0.327 / 0.726).

Statistical analysis revealed a significant interaction of group and timepoint: [GEE, Wald χ^2 (4, N = 82) = 10.277, p = 0.036]. In addition, there was a main effect of group [Wald χ^2 (2, N = 82) = 11.446, p = 0.003] and timepoint [Wald χ^2 (2, N = 82) = 28.633, p < 0.001]. There were no significant differences between the GCaMP and the PBS group at any of the timepoints (baseline: discrimination index, [mean + standard deviation] 0.14 ± 0.4 vs. 0.26 ±0.4, p = 1.000; injection: 0.62 ± 1.4 vs. 0.63 ± 0.1, p = 1.000; implant: 0.27 ± 0.3 vs. 0.18 ± 0.2, p = 1.000). There was no difference between the GCaMP and the control group at baseline (0.14 ± 0.4 vs. 0.26 ±0.4, p = 1.000) and after implantation (0.27 ± 0.3 vs. 0.18 ± 0.2, p = 0.15). However, after injection the GCaMP group learnt better than the control group (0.62 ± 1.4 vs. 0.63 ± 0.1, p < 0.001). Likewise, when we compared the PBS and the control group, there were no statistical differences at baseline (0.26 ± 0.4 vs. 0.33 ± 0.3, p = 1.000) and after implantation (0.18 ± 0.2 vs. 0.02 ± 0.2, p = 0.916), but after the injection the PBS group learnt the task better than the control group (0.63 ± 0.1 vs. 0.16 ± 0.3, p = 0.002). Within-subjects comparisons of timepoints showed a difference in NOR in the GCaMP [Wald χ^2 (2, N = 40) = 32.350, p < 0.001] and in the PBS group [Wald χ^2 (2, N = 18) = 25.024, p < 0.001] but not in the control [Wald χ^2 (2, N = 24) = 5.534, p = 0.063] group. In the GCaMP group, learning was better after injection (0.62 ± 0.14) than at baseline (0.14 ± 0.44, p < 0.001) or after implantation (0.27 ± 0.30, p < 0.001), and in the PBS group a difference was found between injection and implantation (injection vs. implant: 0.63 ± 0.05 vs. 0.18 ± 0.07, p < 0.001).

To conclude, neither the injection nor the lens implantation had an adverse effect on performance in the NOR task.

3.3. There were no group differences in the object-location task at any time point

To test spatial memory, we conducted the OL task. Results are visualized in Fig. 2E. One GCaMP mouse was excluded from the analyses because of low interest in exploring the objects. The GCaMP group (n = 13) showed learning (relative preference for the moved object) at baseline (One-sample Wilcoxon signed-rank test, Z = 2.06, p = 0.039) while the PBS group (n = 6) and the control group (n = 8) did not (Z = 0.53/0.98, p = 0.599/0.327). After injection, none of the groups indicated a preference for the moved object (GCaMP/PBS/control: Z = 1.50/1.36/0.00, p = 0.133/0.173/1.000), but after implantation mice in all groups learnt the task (GCaMP/PBS/control: Z = 2.93/2.20/2.24, p = 0.003/0.028/0.025).

Statistical analysis revealed no interaction (GEE: group x timepoint interaction: Wald χ^2 (4, N = 79) = 4.359, p = 0.360) nor main effect for the group (Wald χ^2 (2, N = 79) = 1.098, p = 0.577), but a main effect for the timepoint (GEE, Wald χ^2 (2, N = 79) = 9.689, p = 0.008) was found. A follow-up analysis revealed that there was a statistically significant difference between injection and implantation [Wald χ^2 (2, N = 79) = 9.689, p = 0.002] in all three groups. The GCaMP and the PBS group showed enhanced learning after implantation (injection vs. implant: GCaMP: 0.10 ± 0.1 vs. 0.37 ± 0.1; PBS: 0.12 ± 0.1 vs. 0.25 ± 0.1), whereas the opposite was detected in the control group (0.05 ± 0.1 vs. 0.33 ± 0.1). That is, the surgical operations had no negative impact on performance in the OL task.

3.4. Adult hippocampal neurogenesis was lesser in the GCaMP group compared to the PBS group

Results on GCaMP/GF expression and AHN are summarized in Fig. 3. Finally, 10 mice survived for the necropsy, of which one GCaMP mouse had extreme GF intensity and AHN values and was therefore excluded from the analyses. In the GCaMP group (n = 9), GCaMP was expressed in the granule cell layer and hilus of the injected dorsal DG, and expectedly the mean GF intensity was many folds higher in the operated hippocampus compared to the intact hippocampus (Fig. 3A) (Z = −2.66, p = 0.008). There was a significant difference in the mean GF intensity between the GCaMP group and the PBS group (n = 6) in the operated hippocampus (5.34 vs. 0.00 arbitrary units, U = 0.00, p = 0.001) but also in the intact hippocampus (0.85 vs. 0.00 arbitrary units, U = 0.00, p = 0.001).

We quantified AHN from the granule cell layer and hilus in both hemispheres (Figs. 3B and 3C). In the GCaMP group, we observed ~40% less DCX-positive cells in the operated dorsal hippocampus compared to the intact, contralateral hippocampus (Z = −2.67, p = 0.008), confirming the negative impact of the surgical operations on AHN. In contrast, in PBS mice, there was no difference in the number of DCX-positive cells between the hemispheres (Z = −0.94, p = 0.345). Furthermore, the GCaMP group had less DCX-positive cells in the operated hippocampus than the PBS group (12 vs. 38 cells, U = 6.50, p = 0.016). Although we used only one titer of AAV in the GCaMP group, we calculated the correlation between the GF intensity and AHN. It turned out that GF intensity did not correlate with the number of DCX-positive cells in either the GCaMP group (r_s = 0.083, p = 0.843) or in the PBS group (r_s = 0.594, p = 0.300) (Fig. 3 C).

4. Discussion

In this study, we assessed whether surgical procedures required for calcium imaging of the DG would have adverse effects on AHN and the behavior of mice. We did not detect increase in anxiety-related behavior, and the procedures impaired neither object-recognition nor spatial learning after the operations, even though a decrease in AHN was observed in the dorsal DG ipsilateral to the AAV.CamKII.GCaMP6 injection. As expected, performance in the learning tasks improved as a function of repetition. Taken together, our results indicate that the two hippocampi form plastic networks that can reorganize after partial, unilateral damage and can still support (at least spatial and episodic) memory functions. These results can be utilized in planning invasive studies, in which the target is the hippocampus.

Although dorsal hippocampal lesions in rodents have been linked to behavioral changes such as increased activity in novel environments [12] and disruption of behavioral habituation [9], in this study we did not detect such changes. seemed to habituate to the environment better than the control mice, measured as a decrease in rearing activity. However, one must keep in mind that there is no unambiguous interpretation for rearing, as it has been related to both exploration activity and anxiety ([7]; see also: [39]). Thus, it is also possible that the surgical operations negatively impacted the wellbeing of the mice, decreasing

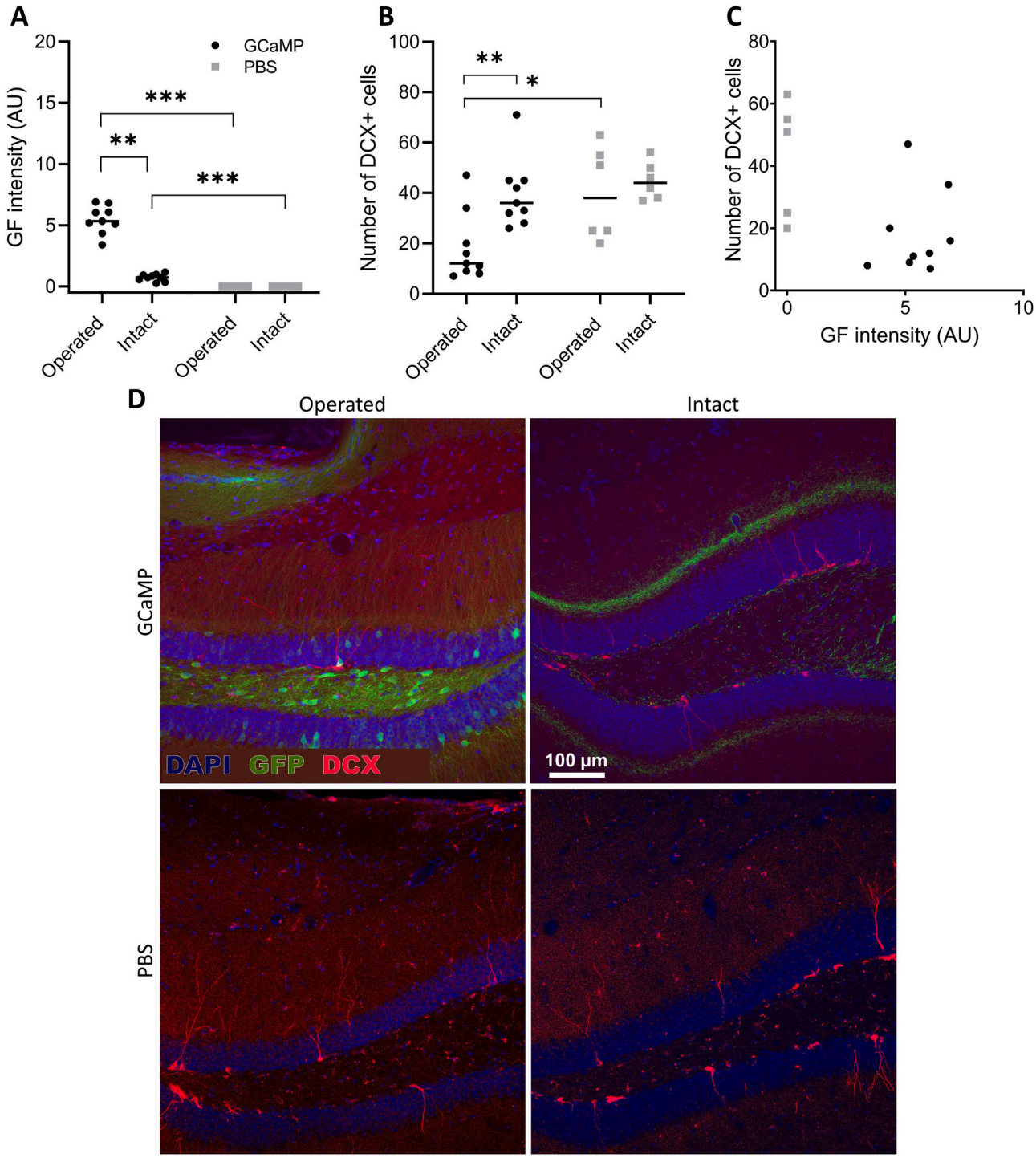

Fig. 3. AAV.CamKII.GCaMP6 decreased AHN in the DG of the injected hippocampus. A) The green fluorescence (GF) intensity (mean + SD) in the GCaMP group was significantly higher in the operated hippocampus compared to the intact hippocampus and to the PBS group. The GF intensity was analyzed using confocal microscope (Zeiss LSM 700, 10x/NA 0.45) and QuPath® software. B) A decrease in DCX-positive cells was detected in the operated hippocampus of the GCaMP group. DCX+ cells were immunolabeled with fluorescent antibodies, and the number of DCX+ cells is a sum value from three hippocampal sections 1.06 – 3.08 posterior to bregma. In both panels, vertical lines describe the mean values. C) The correlation (ns) between mean GF intensity and the number of DCX-positive cells. Representative images of D) DCX-positive cells (red), nuclei (DAPI-staining, blue), and GCaMP expression (green) in the two dentate gyri of mice from the GCaMP group (above) and from the PBS group (below). The scale is the same in all histological images. Asterisks refer to statistically significant differences in Wilcoxon signed-rank test and Mann-Whitney U test: $p < 0.050$ (*), $p \leq 0.01$ (**) and $p < 0.001$ (***).

their willingness to explore the environment. Further, the time spent in the center of the arena decreased in the GCaMP group and only after the injection, suggesting that the viral construct injection could indeed cause an increase in anxiety-related behavior. Since there were no group differences after the injection and implantation, a more likely explanation to the different behavior of the GCaMP group is the use of different floor color and texture in the arena during the baseline test. Thus, it can be concluded that unilateral surgical operations of the hippocampus, needed for calcium imaging, may impact activity of the mice but have only a modest effect (if all) on anxiety.

It is known that in humans bilateral but not unilateral hippocampal lesions cause a severe memory impairment [35]. As expected, in our study invasive procedures targeted to one hippocampus did not impair object recognition. In fact, both GCaMP and PBS groups improved in object recognition over time, whereas the control group did not. This is in line with previous studies reporting that hippocampal lesions do not impair object discrimination [13,27] but might even enhance non-spatial learning by eliminating interference from spatial cues [34]. In contrast, numerous studies suggest that bilateral hippocampal lesions impair spatial memory [12,26,27]. Our unilateral procedures did not impair learning in the object-location task, and we found no significant behavioral differences between mice operated on the left vs. the right hippocampus (results not shown), suggesting that either one of the two hippocampi is sufficient for supporting learning and memory. In fact, all groups improved performance throughout the experiment, suggesting that the ability to learn spatial information was enhanced with practice [29]. In conclusion, unilateral procedures needed for hippocampal imaging did not impair learning and memory. Nevertheless, further studies are needed to find out whether the unilateral operations impact learning in more complex tasks such as pattern separation involving the DG [10, 32].

We found that in comparison to the PBS group, mice in the GCaMP group had less adult-born new neurons in the operated hippocampus 6 months after the injection. We detected no correlation between the AHN and GF intensity, suggesting that variations in the GCaMP expression do not linearly associate with AHN. The dose of the viral vector construct that we used was lower than that used by Johnston and colleagues (2021) and most other groups targeting the DG [2,41]. Thus, it could be hypothesized that the effect on AHN in those studies would be even more detrimental. However, since the loss in AHN is seen mostly when directly targeting the DG and not the other areas of the hippocampus [16,20], in studies concentrating on CA1 or CA3 higher viral doses could likely be used without disturbing AHN. Compared to most other studies, our expression time was relatively long (~6 months), allowing GCaMP to accumulate over time. For example, Johnston et al. [20] reported only a modest decrease in AHN one week after the injection using a dose ~100 times higher than us. This implies that time is of essence when evaluating possible effects on AHN. To sum up, AAV.CaMKII.GCaMP6 reduces AHN. To minimize this effect, the duration of the experiment, the viral vector dose, and the injection strategy should be carefully chosen.

As discussed above, learning was not impaired in the GCaMP group compared to the control groups. Previously, it has been reported that even partial bilateral ablation of adult-born DG granule cells can impair object-location memory in rats [17] [see also [23]]. However, here the decrease in AHN was unilateral. Because no changes in behavior were evident, our current results suggest that the intact, unoperated hippocampus can functionally compensate for the loss of AHN in the other hippocampus. We must underline that in the current study the interval between the behavioral tasks and the DCX-staining was ~6 months, and we have no information about the AHN during or right after the behavioral tasks. Yet, it seems plausible that AHN ablation occurred already after one week from the injection [20], and the effects of AHN ablation on behavior should have been evident not more than two weeks later [17]. Based on this, we would have expected to see changes in behavior latest in the 3rd round of the tasks (after implantation), that is, ~4 weeks after the injection. To conclude, unilateral partial ablation of AHN does not seem to affect object recognition or spatial learning in mice.

A limitation of this study was that we did not inspect how the miniature microscope needed for calcium imaging affects behavior of the mice during the tasks. The camera weighs ~2 g and is connected to the data acquisition unit with a cord. It could hinder movement of the animal and thus affect exploration. In addition, because AHN was decreased even with a relatively small dose of the viral vector, alternative injection strategies, for example a retrograde AAV vector into the CA3 [16,20] could be considered at least in studies in which higher doses are needed. In further studies, also more detailed inspection of structural changes such as changes in the thickness of the hilus or the suprapyramidal blade of the DG should be carried out.

In conclusion, despite the persistent decrease in AHN, unilateral surgical operations needed for calcium imaging did not impair recognition memory or spatial learning in adult male mice. Thus, our results suggest that in vivo imaging can be safely used to, for example, correlate patterns of calcium activity with learned behavior. One should consider that the defects on the operated side might be functionally compensated by the (hippocampus in the) contralateral hemisphere.

Funding

This work was supported by the Academy of Finland (grant no. 321522 and 355392 to MSN and grant no. 316966 to Markku Penttonen).

CRediT authorship contribution statement

Veera Puumalainen: Visualization, Writing – original draft, Investigation. **Suvi-Maaria Lehtonen:** Visualization, Writing – original draft, Formal analysis, Investigation. **Miriam S. Nokia:** Conceptualization, Funding acquisition, Supervision, Writing – review & editing, Methodology, Resources. **Sanna Lensu:** Conceptualization, Supervision, Writing – review & editing.

Declaration of Competing Interest

None.

Data availability

Data will be made available on request.

Acknowledgements

We would like to thank Sunna Karjalainen and Roosa-Mariia Hooli for help with data collection and analysis, Dr. Arto Lipponen for technical assistance, and Joona Muotka for advice on statistical analyses. We also thank Eliisa Kiukkanen, Aija Leppänen, and all the other staff for taking good care of the animals.

References

[1] M. Allegra, L. Posani, R. Gómez-Ocádiz, C. Schmidt-Hieber, Differential relation between neuronal and behavioral discrimination during hippocampal memory encoding, Neuron *108* (6) (2020) 1103–1112.e6, https://doi.org/10.1016/j.neuron.2020.09.032.

[2] C. Anacker, V.M. Luna, G.S. Stevens, A. Millette, R. Shores, J.C. Jimenez, B. Chen, R. Hen, Hippocampal neurogenesis confers stress resilience by inhibiting the ventral dentate gyrus, Nature *559* (7712) (2018) 98–102, https://doi.org/10.1038/s41586-018-0262-4.

[3] D.F. Aschauer, S. Kreuz, S. Rumpel, Analysis of transduction efficiency, tropism and axonal transport of AAV serotypes 1, 2, 5, 6, 8 and 9 in the mouse brain, PLoS ONE *8* (9) (2013) e76310, https://doi.org/10.1371/journal.pone.0076310.

[4] P. Bankhead, M.B. Loughrey, J.A. Fernández, Y. Dombrowski, D.G. McArt, P. D. Dunne, S. McQuaid, R.T. Gray, L.J. Murray, H.G. Coleman, J.A. James, M. Salto-Tellez, P.W. Hamilton, QuPath: open source software for digital pathology image analysis, Sci. Rep. *7* (1) (2017) 16878, https://doi.org/10.1038/s41598-017-17204-5.

[5] S.D. Berry, R.F. Thompson, Medial septal lesions retard classical conditioning of the nictitating membrane response in rabbits, Science *205* (4402) (1979) 209–211, https://doi.org/10.1126/science.451592.

[6] E.J. Bubb, C. Metzler-Baddeley, J.P. Aggleton, The cingulum bundle: anatomy, function, and dysfunction, Neurosci. Biobehav. Rev. *92* (2018) 104–127, https://doi.org/10.1016/j.neubiorev.2018.05.008.

[7] U.A.G. Carnevale, E. Vitullo, A.G. Sadile, Post-trial NMDA receptor allosteric blockade differentially influences habituation of behavioral responses to novelty in the rat, Behav. Brain Res. *39* (2) (1990) 187–195, https://doi.org/10.1016/0166-4328(90)90104-M.

[8] A. Carrier-Ruiz, Y. Sugaya, D. Kumar, P. Vergara, I. Koyanagi, S. Srinivasan, T. Naoi, M. Kano, M. Sakaguchi, Calcium imaging of adult-born neurons in freely moving mice, STAR Protoc. *2* (1) (2021) 100238, https://doi.org/10.1016/j.xpro.2020.100238.
[9] B.J. Clark, D.J. Hines, D.A. Hamilton, I.Q. Whishaw, Movements of exploration intact in rats with hippocampal lesions, Behav. Brain Res. *163* (1) (2005) 91–99, https://doi.org/10.1016/j.bbr.2005.04.007.
[10] C.D. Clelland, M. Choi, C. Romberg, G.D. Clemenson, A. Fragniere, P. Tyers, S. Jessberger, L.M. Saksida, R.A. Barker, F.H. Gage, T.J. Bussey, A functional role for adult hippocampal neurogenesis in spatial pattern separation, Science *325* (5937) (2009) 210–213, https://doi.org/10.1126/science.1173215.
[11] S.J. Cohen, A.H. Munchow, L.M. Rios, G. Zhang, H.N. Ásgeirsdóttir, R. W. Stackman, The rodent hippocampus is essential for nonspatial object memory, Curr. Biol. *23* (17) (2013) 1685–1690, https://doi.org/10.1016/j.cub.2013.07.002.
[12] G.M. Dillon, X. Qu, J.N. Marcus, J.-C. Dodart, Excitotoxic lesions restricted to the dorsal CA1 field of the hippocampus impair spatial memory and extinction learning in C57BL/6 mice, Neurobiol. Learn. Mem. *90* (2) (2008) 426–433, https://doi.org/10.1016/j.nlm.2008.05.008.
[13] C.A. Duva, S.B. Floresco, G.R. Wunderlich, T.L. Lao, J.P.J. Pinel, A.G. Phillips, Disruption of spatial but not object-recognition memory by neurotoxic lesions of the dorsal hippocampus in rats, Behav. Neurosci. *111* (6) (1997) 1184–1196, https://doi.org/10.1037/0735-7044.111.6.1184.
[14] A. Ennaceur, One-trial object recognition in rats and mice: methodological and theoretical issues, Behav. Brain Res. *215* (2) (2010) 244–254, https://doi.org/10.1016/j.bbr.2009.12.036.
[15] A. Ennaceur, J. Delacour, A new one-trial test for neurobiological studies of memory in rats. 1: behavioral data, Behav. Brain Res. *31* (1) (1988) 47–59, https://doi.org/10.1016/0166-4328(88)90157-X.
[16] S. Ge, E.L.K. Goh, K.A. Sailor, Y. Kitabatake, G. Ming, H. Song, GABA regulates synaptic integration of newly generated neurons in the adult brain, Nature *439* (7076) (2006) 589–593, https://doi.org/10.1038/nature04404.
[17] T. Goodman, S. Trouche, I. Massou, L. Verret, M. Zerwas, P. Roullet, C. Rampon, Young hippocampal neurons are critical for recent and remote spatial memory in adult mice, Neuroscience *171* (3) (2010) 769–778, https://doi.org/10.1016/j.neuroscience.2010.09.047.
[18] R.W. Herzog, Immune responses to AAV capsid: are mice not humans after all, Mol. Ther. *15* (4) (2007) 649–650, https://doi.org/10.1038/sj.mt.6300123.
[19] P. Jercog, T. Rogerson, M.J. Schnitzer, Large-scale fluorescence calcium-imaging methods for studies of long-term memory in behaving mammals, Cold Spring Harb. Perspect. Biol. *8* (5) (2016) a021824, https://doi.org/10.1101/cshperspect.a021824.
[20] S. Johnston, S.L. Parylak, S. Kim, N. Mac, C. Lim, I. Gallina, C. Bloyd, A. Newberry, C.D. Saavedra, O. Novak, J.T. Gonçalves, F.H. Gage, M. Shtrahman, AAV ablates neurogenesis in the adult murine hippocampus, eLife *10* (2021) e59291, https://doi.org/10.7554/eLife.59291.
[21] M.G. Kaplitt, P. Leone, R.J. Samulski, X. Xiao, D.W. Pfaff, K.L. O'Malley, M. J. During, Long-term gene expression and phenotypic correction using adeno-associated virus vectors in the mammalian brain, Nat. Genet. *8* (2) (1994) 148–154, https://doi.org/10.1038/ng1094-148.
[22] G.W. Kirschen, J. Shen, M. Tian, B. Schroeder, J. Wang, G. Man, S. Wu, S. Ge, Active dentate granule cells encode experience to promote the addition of adult-born hippocampal neurons, J. Neurosci. *37* (18) (2017) 4661–4678, https://doi.org/10.1523/JNEUROSCI.3417-16.2017.
[23] S. Lensu, T. Waselius, E. Mäkinen, H. Kettunen, A. Virtanen, M. Tiirola, M. Penttonen, S. Pekkala, M.S. Nokia, Irradiation of the head reduces adult hippocampal neurogenesis and impairs spatial memory, but leaves overall health intact in rats, Eur. J. Neurosci. *53* (6) (2021) 1885–1904, https://doi.org/10.1111/ejn.15102.
[24] L.A. Martin, F. Hsu, B. Herd, M. Gregg, H. Sample, J. Kaplan, Executive functions in agenesis of the corpus callosum: working memory and sustained attention in the BTBR inbred mouse strain, Brain Behav. *11* (1) (2021) e01933, https://doi.org/10.1002/brb3.1933.
[25] S.M. McMahon, M.B. Jackson, An inconvenient truth: calcium sensors are calcium buffers, Trends Neurosci. *41* (12) (2018) 880–884, https://doi.org/10.1016/j.tins.2018.09.005.
[26] R.G.M. Morris, P. Garrud, J.N.P. Rawlins, J. O'Keefe, Place navigation impaired in rats with hippocampal lesions, Nature *297* (5868) (1982) 681–683, https://doi.org/10.1038/297681a0.
[27] D.G. Mumby, S. Gaskin, M.J. Glenn, T.E. Schramek, H. Lehmann, Hippocampal damage and exploratory preferences in rats: memory for objects, places, and contexts, Learn. Mem. *9* (2) (2002) 49–57, https://doi.org/10.1101/lm.41302.
[28] J. Nakai, M. Ohkura, K. Imoto, A high signal-to-noise Ca2+ probe composed of a single green fluorescent protein, Nat. Biotechnol. *19* (2) (2001) 137–141, https://doi.org/10.1038/84397.
[29] M.S. Nokia, H.M. Sisti, M.R. Choksi, T.J. Shors, Learning to learn: theta oscillations predict new learning, which enhances related learning and neurogenesis, PLoS ONE *7* (2) (2012) e31375, https://doi.org/10.1371/journal.pone.0031375.
[30] R.C. O'Reilly, J.L. McClelland, Hippocampal conjunctive encoding, storage, and recall: Avoiding a trade-off, Hippocampus *4* (6) (1994) 661–682, https://doi.org/10.1002/hipo.450040605.
[31] G. Paxinos, K.B.J. Franklin. The Mouse Brain in Stereotaxic Coordinates, second ed., Academic Press, San Diego, 2004.
[32] A. Sahay, K.N. Scobie, A.S. Hill, C.M. O'Carroll, M.A. Kheirbek, N.S. Burghardt, A. A. Fenton, A. Dranovsky, R. Hen, Increasing adult hippocampal neurogenesis is sufficient to improve pattern separation, Nature *472* (7344) (2011) 466–470, https://doi.org/10.1038/nature09817.
[33] A. Sahay, D.A. Wilson, R. Hen, Pattern separation: a common function for new neurons in hippocampus and olfactory bulb, Neuron *70* (4) (2011) 582–588, https://doi.org/10.1016/j.neuron.2011.05.012.
[34] D.J. Sanderson, J.N.P. Rawlins, R.M.J. Deacon, C. Cunningham, C. Barkus, D. M. Bannerman, Hippocampal lesions can enhance discrimination learning despite normal sensitivity to interference from incidental information, Hippocampus *22* (7) (2012) 1553–1566, https://doi.org/10.1002/hipo.20995.
[35] W.B. Scoville, B. Milner, Loss of recent memory after bilateral hippocampal lesions, J. Neurol. Neurosurg. Psychiatry *20* (1) (1957) 11–21, https://doi.org/10.1136/jnnp.20.1.11.
[36] L.R. Squire, Declarative and nondeclarative memory: multiple brain systems supporting learning and memory, J. Cogn. Neurosci. *4* (3) (1992) 232–243, https://doi.org/10.1162/jocn.1992.4.3.232.
[37] F. Stefanini, L. Kushnir, J.C. Jimenez, J.H. Jennings, N.I. Woods, G.D. Stuber, M. A. Kheirbek, R. Hen, S. Fusi, A distributed neural code in the dentate gyrus and in CA1, e4, Neuron *107* (4) (2020) 703–716, https://doi.org/10.1016/j.neuron.2020.05.022.
[38] N.A. Steinmetz, C. Buetfering, J. Lecoq, C.R. Lee, A.J. Peters, E.A.K. Jacobs, P. Coen, D.R. Ollerenshaw, M.T. Valley, S.E.J. De Vries, M. Garrett, J. Zhuang, P. A. Groblewski, S. Manavi, J. Miles, C. White, E. Lee, F. Griffin, J.D. Larkin, K. D. Harris, Aberrant cortical activity in multiple GCaMP6-expressing transgenic mouse lines, ENEURO.0207-17.2017, Eneuro *4* (5) (2017), https://doi.org/10.1523/ENEURO.0207-17.2017.
[39] O. Sturman, P.-L. Germain, J. Bohacek, Exploratory rearing: a context- and stress-sensitive behavior recorded in the open-field test, Stress *21* (5) (2018) 443–452, https://doi.org/10.1080/10253890.2018.1438405.
[40] E. Tulving, D.M. Thomson, Encoding specificity and retrieval processes in episodic memory, Psychol. Rev. *80* (5) (1973) 352–373, https://doi.org/10.1037/h0020071.
[41] N.I. Woods, F. Stefanini, D.L. Apodaca-Montano, I.M.C. Tan, J.S. Biane, M. A. Kheirbek, The dentate gyrus classifies cortical representations of learned stimuli, Neuron *107* (1) (2020) 173–184.e6, https://doi.org/10.1016/j.neuron.2020.04.002.